



DEPARTMENT OF PLANNING, INDUSTRY & ENVIRONMENT

Climate change impacts in the NSW and ACT Alpine region

Impacts of extreme rainfall on soil erosivity and hillslope erosion



© 2019 State of NSW and Department of Planning, Industry and Environment

With the exception of photographs, the State of NSW and Department of Planning, Industry and Environment are pleased to allow this material to be reproduced in whole or in part for educational and non-commercial use, provided the meaning is unchanged and its source, publisher and authorship are acknowledged. Specific permission is required for the reproduction of photographs.

The Department of Planning, Industry and Environment (DPIE) has compiled this report in good faith, exercising all due care and attention. No representation is made about the accuracy, completeness or suitability of the information in this publication for any particular purpose. DPIE shall not be liable for any damage which may occur to any person or organisation taking action or not on the basis of this publication. Readers should seek appropriate advice when applying the information to their specific needs.

All content in this publication is owned by DPIE and is protected by Crown Copyright, unless credited otherwise. It is licensed under the [Creative Commons Attribution 4.0 International \(CC BY 4.0\)](#), subject to the exemptions contained in the licence. The legal code for the licence is available at [Creative Commons](#).

DPIE asserts the right to be attributed as author of the original material in the following manner: © State of New South Wales and Department of Planning, Industry and Environment 2019.

Cover photo: Winter landscape in Kosciuszko National Park. John Spencer/DPIE

This report should be cited as:

Zhu EQ and Yang X 2019, *Climate change impacts in the NSW and ACT Alpine region: Impacts of extreme rainfall on soil erosivity and hillslope erosion*, NSW Department of Planning, Industry and Environment, Sydney, Australia.

Published by:

Environment, Energy and Science
Department of Planning, Industry and Environment
59 Goulburn Street, Sydney NSW 2000
PO Box A290, Sydney South NSW 1232
Phone: +61 2 9995 5000 (switchboard)
Phone: 1300 361 967 (Environment, Energy and Science enquiries)
TTY users: phone 133 677, then ask for 1300 361 967
Speak and listen users: phone 1300 555 727, then ask for 1300 361 967
Email: info@environment.nsw.gov.au
Website: www.environment.nsw.gov.au

Report pollution and environmental incidents
Environment Line: 131 555 (NSW only) or info@environment.nsw.gov.au
See also www.environment.nsw.gov.au

ISBN 978 1 922318 16 9
EES 2020/0021
January 2020

Find out more about your environment at:

www.environment.nsw.gov.au

Contents

| | |
|---|-----|
| List of shortened forms | v |
| Summary of findings | vii |
| 1. Introduction | 1 |
| 1.1 Background | 1 |
| 1.2 Objectives | 2 |
| 1.3 Outputs | 2 |
| 2. Method | 3 |
| 2.1 Source of data | 3 |
| 2.2 Quality control | 6 |
| 2.3 Data storage and access | 6 |
| 3. Results | 6 |
| 3.1 Correlation between extreme rainfall indices and rainfall erosivity | 6 |
| 3.2 Annual and seasonal rainfall erosivity | 8 |
| 3.3 Future change in rainfall erosivity | 9 |
| 3.4 Impact of snowmelt on erosivity | 12 |
| 3.5 Hillslope erosion projection and changes | 13 |
| 4. Discussion | 17 |
| 4.1 Extra rainfall erosivity in spring | 17 |
| 4.2 High risk areas | 17 |
| 4.3 Limitations and further research | 17 |
| 5. Conclusion | 17 |
| 6. References | 18 |

List of tables

| | | |
|---------|---|----|
| Table 1 | The selected six extreme rainfall indices and their definitions | 4 |
| Table 2 | Seasonal comparison between extreme rainfall indices, Rx1day and Rx5day, and their correlation with rainfall erosivity | 7 |
| Table 3 | Annual and seasonal mean values of rainfall erosivity in the baseline, near future and far future periods across the study area | 8 |
| Table 4 | Changes in mean annual and seasonal rainfall erosivity (%) in the near future (2020 to 2039) and far future (2060 to 2079) | 10 |
| Table 5 | Mean and maximum annual erosion values ($t\ ha^{-1}\ yr^{-1}$) across the study area in the baseline (1990 to 2009), near future (2020 to 2039) and far future (2060 to 2079) periods | 15 |
| Table 6 | Changes (%) in mean annual and seasonal erosion values across the study area in the near future (2020 to 2039) and far future (2060 to 2079) | 15 |

List of figures

| | | |
|-----------|--|----|
| Figure 1 | The domain of the snow projections, the NSW and ACT Alpine region and the boundaries of the state planning regions within the study area in NSW | 1 |
| Figure 2 | Correlation coefficients between different extreme rainfall indices (refer to Table 1) and rainfall erosivity (a) and erosion (b) for the baseline period (1990 to 2009), near future (2020 to 2039) and far future (2060 to 2079) | 7 |
| Figure 3 | Relationship between mean annual erosivity and Rx5day index | 8 |
| Figure 4 | Mean annual rainfall erosivity in the baseline (1990 to 2009), near future (2020 to 2039) and far future (2060 to 2079) periods, compared with that calculated from BoM gridded rainfall in the 1990 to 2009 baseline period | 9 |
| Figure 5 | Changes in mean annual rainfall erosivity (%) in the near future (2020 to 2039) relative to the 1990 to 2009 baseline period | 10 |
| Figure 6 | Changes in mean annual rainfall erosivity (%) in the far future (2060 to 2079) relative to the 1990 to 2009 baseline period | 11 |
| Figure 7 | Changes in mean seasonal rainfall erosivity (%) in the near future (2020 to 2039) relative to the 1990 to 2009 baseline period | 11 |
| Figure 8 | Changes in mean seasonal rainfall erosivity (%) in the far future (2060 to 2079) relative to the 1990 to 2009 baseline period | 12 |
| Figure 9 | Projected change (%) in rainfall erosivity with and without snowmelt for the baseline (1990 to 2009), near future (2020 to 2039) and far future (2060 to 2079) periods | 13 |
| Figure 10 | Projected hillslope erosion risk ($t\ ha^{-1}\ yr^{-1}$) for the 1990 to 2009 baseline period | 13 |
| Figure 11 | Projected hillslope erosion risk ($t\ ha^{-1}\ yr^{-1}$) for the near future (2020 to 2039) | 14 |
| Figure 12 | Projected hillslope erosion risk ($t\ ha^{-1}\ yr^{-1}$) for the far future (2060 to 2079) | 14 |
| Figure 13 | Projected hillslope erosion risk across the study area for the baseline (1990 to 2009), the near future (2020 to 2039) and the far future (2069 to 2079) periods | 16 |
| Figure 14 | The C, K and LS factors of RUSLE across the study area | 16 |

List of shortened forms

| | |
|---------|--|
| ACT | Australian Capital Territory |
| BoM | Australian Bureau of Meteorology |
| CSIRO | Commonwealth Scientific and Industrial Research Organisation |
| DEM | Digital Elevation Model |
| DJF | December January February |
| DPIE | Department of Planning, Industry and Environment |
| ERIs | extreme rainfall indices |
| GCM | Global Climate Model |
| GIS | geographic information system |
| JJA | June July August |
| LS | slope-steepness factor |
| MAM | March April May |
| MCAS-S | Multi-Criteria Analysis Shell for Spatial Decision Support |
| MLR | multiple linear regression |
| MM | Murray-Murrumbidgee state planning region |
| NARClIM | NSW/ACT Regional Climate Modelling project |
| NSW | New South Wales |
| OEH | Office of Environment and Heritage |
| RCM | Regional Climate Model |
| RR | daily precipitation on a specified day |
| RUSLE | revised universal soil loss equation |
| SET | Southeast and Tablelands state planning region |
| SON | September October November |
| SRTM | Shuttle Radar Topography Mission |

Summary of findings

Impacts of extreme rainfall on soil erosivity and hillslope erosion

1. Extreme rainfall impacts erosivity and hillslope erosion.
2. Extreme rainfall indices can be used to predict potential high-risk areas of rainfall erosivity and hillslope erosion. There is a good linear relationship between the 5-day maximum precipitation index (Rx5Day) and rainfall erosivity ($R^2 > 0.81$).
3. A snowmelt adjusted erosivity model and snow cover data have been applied in the Alpine region.
4. Rainfall erosivity and hillslope erosion in the NSW Alpine region are projected to increase by 2–8% in the near future (2020 to 2039), and 8–18% in the far future (2060 to 2079), even if the groundcover is maintained at the current level.
5. The change in rainfall erosivity and erosion risk is highly uneven in both location and season. Summer is projected to have the highest erosion risk with an increase of about 25% in the next 20 to 50 years.
6. The highest erosion risk area within the study area is projected to be in the South East and Tablelands (SET, maximum rate: $19.95 \text{ t ha}^{-1} \text{ yr}^{-1}$), but on average, the ACT has the highest erosion rate, which is above 1.3 tonnes per hectare per year in all periods. The maximum rainfall erosivity in the region is projected to be in SET with 1233.87 megajoule millimetres per hectare per hour per year in the far future.
7. The impact of snowmelt on rainfall erosivity and erosion needs to be considered in the Alpine region in both the baseline and near future periods. The snowmelt in spring can increase the erosivity by about 13–24% in the Alpine area; however, with the projected temperature rise and projected decreases in snow cover, the snowmelt impact on erosivity and erosion can largely be ignored in the far future.

1. Introduction

1.1 Background

The New South Wales (NSW) and Australian Capital Territory (ACT) Alpine region is located in the south-eastern corner of mainland Australia and is the highest mountain range in Australia. Though it comprises only about 0.16% of Australia in size, it is an important region for ecosystems, biodiversity, energy generation and winter tourism. It forms the southern end of the Great Dividing Range, covering a total area of 1.64 million hectares that extend over 500 kilometres. The highest peak, Mount Kosciuszko, rises to an altitude of 2228 metres.

This report is part of a larger project delivered by the NSW Department of Planning, Industry and Environment on the various impacts from climate change on the NSW and ACT Alpine region, hereafter referred to as the Alpine region. The full study region covers the Murray-Murrumbidgee region (MM), South East and Tablelands (SET) and the ACT, bordering the Victorian border in the south (Figure 1).

The Alpine region is vulnerable to climate change. Observations have shown substantial changes in precipitation and temperature for this area (Di Luca et al. 2018), which have already impacted biodiversity and ecosystems (Hughes 2011). In 2014, the NSW/ACT Regional Climate Modelling (NARClIM) project was delivered. Climate snapshots for each of the 11 NSW planning regions and the ACT were developed to demonstrate observed and projected climate change; however, the snapshots only show changes for some variables and focus on each planning region.

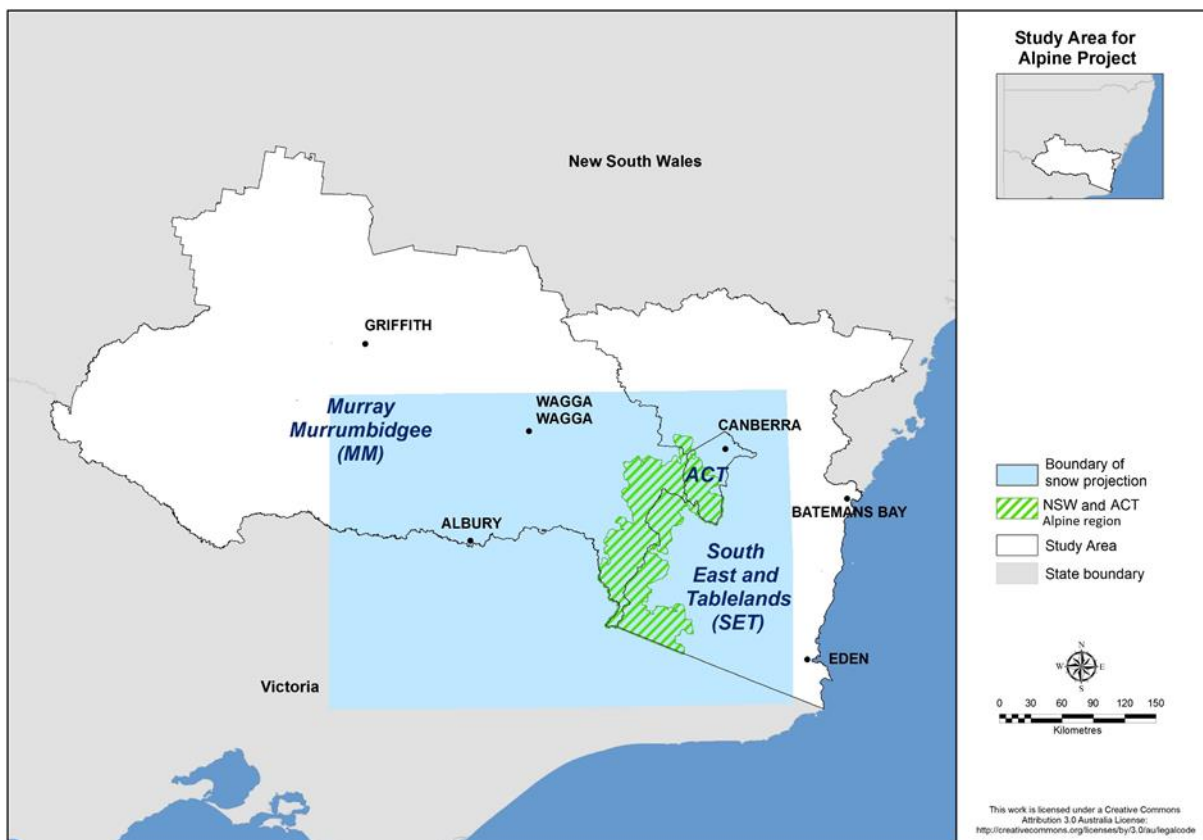


Figure 1 The domain of the snow projections, the NSW and ACT Alpine region and the boundaries of the state planning regions within the study area in NSW

1.2 Objectives

Climate extremes have attracted global attention in recent decades because they are often more important to natural and human systems than the mean values of climate variables (Cruse et al. 2006). Research on rainfall extremes reports significant changes in percentiles and frequency of extreme events, and the magnitude and sign of the changes varies with season and region (Alexander et al. 2007; CSIRO & BoM 2015). Hillslope erosion rates may be expected to change in response to changes in climate; for example, change in the erosive power of rainfall (e.g. Nearing et al. 2004). Hillslope erosion occurs mostly during severe storms or extreme events. Large and erosive storms are more variable than annual rainfall totals. Trends and changes in erosive storms or rainfall extremes are therefore much more important but also difficult to detect, when compared with rainfall totals.

The downscaled 10 kilometre rainfall projections from NARClIM (Evans et al. 2014a) have become available for this project for a baseline period (1990 to 2009), near future period (2020 to 2039) and far future period (2060 to 2079). The NARClIM projected rainfall and snow in these three periods and 12 ensembles (four Global Climate Models (GCMs) and three Regional Climate Models (RCMs)) (Evans et al. 2014a) were used to calculate extreme rainfall indices (ERIs). The indices in the baseline period (1990 to 2009) were compared to those calculated from rainfall data from the Bureau of Meteorology (BoM).

The objectives of this study were to: i) model and predict the changes in rainfall extremes and the impacts on hillslope erosion risk across the Alpine region based on the NARClIM projections; and ii) predict locations and times with high erosion risk across the study area. Outcomes from this study include: i) maps of six ERIs; ii) time-series hillslope erosion risk maps; iii) impact assessment of extreme rainfall on hillslope erosion; iv) reports; and v) spatial data layers in a geographic information system (GIS). These outcomes will assist long-term climate change adaptation and regional planning in the Alpine region.

In this study, we examined the relationship between ERI and rainfall erosivity across the study area. This relationship was used as an approximation of rainfall erosivity and compared with estimates from the previous studies (Yang & Yu 2015; Yang et al. 2016). The projected rainfall erosivity was used to estimate hillslope erosion based on the revised universal soil loss equation (RUSLE) along with the slope-steepness factor and the soil erodibility factor (Renard et al. 1997). Rainfall erosivity was calibrated using the snowmelt runoff in spring (September, October and November – SON). Time-series (monthly and annual) rainfall extremes and erosion risk for the study area for each of the 20-year periods have been produced and spatially interpolated to a high spatial resolution of 100 metres in GIS using a spline interpolation method.

Statistical tests were used to quantify the spatial and temporal changes in rainfall extremes and the impacts on hillslope erosion across the study area and its subregions. The time-series maps for each of the 20-year periods were used to identify the high erosion risk seasons and areas. Automated GIS scripts were developed to calculate the time-series rainfall erosivity and hillslope erosion so the processes of large quantity NARClIM data are realistic, repeatable and portable.

1.3 Outputs

| Output | Details | Key user |
|-------------------------|---|---------------------------------------|
| Report | Impact assessment of extreme rainfall on hillslope erosion | Researchers |
| Data (GIS layers) | Extreme rainfall indices (six) Monthly and annual rainfall erosivity and hillslope erosion risk maps for all three periods (60 years) Seasonal and annual rainfall erosivity and erosion change (%) in the near future and far future | NSW National Parks & Wildlife Service |
| Maps | Map layouts of the above data (in JPEG and GeoTiff) | Councils, etc. |

2. Method

2.1 Source of data

NARCLiM simulations from four Coupled Model Intercomparison Project phase 3 (CMIP3) Global Climate Models (GCMs) were used to drive three Regional Climate Models (RCMs) to form a 12-member GCM/RCM ensemble (Evans et al. 2014a). The four selected GCMs are MIROC3.2, ECHAM5, CCCMA3.1 and CSIRO-MK3.0. For future projections, the Special Report on Emissions Scenarios (SRES) business-as-usual A2 scenario was used (IPCC 2000). The three selected RCMs are three physics scheme combinations of the Weather Research and Forecasting (WRF) model. Each simulation consists of three 20-year runs (1990 to 2009, 2020 to 2039, and 2060 to 2079). The four GCMs were chosen based on a number of criteria: i) adequate performance when simulating historic climate; ii) most independent; iii) cover the largest range of plausible future precipitation and temperature changes for Australia. The three RCMs correspond to three different physics scheme combinations of the WRF V3.3 model (Skamarock et al. 2008), which were also chosen for adequate skill and error independence, following a comprehensive analysis of 36 different combinations of physics parameterisations over eight significant East Coast Lows (ECLs) (Evans et al. 2012; Ji et al. 2014). For the selected three RCMs, the WRF Double Moment 5-class (WDM5) microphysics scheme and NOAA land surface scheme are used in all cases. Refer to Evans et al. (2014a) for more details on each physics scheme.

We acknowledge that the results are model dependent (as all model studies are) but through the use of this carefully selected ensemble we have attempted to minimise this dependence. By using this model selection process, we have shown that it is possible to create relatively small ensembles that are able to reproduce the ensemble mean and variance from the large parent ensemble (i.e. the many GCMs) as well as minimise the overall error (Evans et al. 2013a).

Some initial evaluation of NARCLiM simulations shows that they have strong skill in simulating the precipitation and temperature of Australia, with a small cold bias and overestimation of precipitation on the Great Dividing Range (Evans et al. 2013b; Ji et al. 2016). The differing responses of the different RCMs confirm the utility of considering model independence when choosing the RCMs. The RCM response to large-scale modes of variability also agrees well with observations (Fita et al. 2016). Through these evaluations we found that while there is a spread in model projections, all models perform adequately with no single model performing the best for all variables and metrics. The use of the full ensemble provides a measure of robustness such that any result that is common through all models in the ensemble is considered to have higher confidence.

This study uses the bias-corrected rainfall extremes projections with a spatial resolution of 10 kilometres (Evans et al. 2017) from NARCLiM to estimate the future rainfall erosivity in the Alpine region. Snow projection and daily mean temperature products from NARCLiM were obtained from the Department of Planning, Industry and Environment (DPIE) and University of New South Wales (UNSW) at a 10 kilometre spatial resolution. Snow depth and density simulation for the 60 years were extracted from the snow projections and used to estimate and adjust the snowmelt runoff (Bormann et al. 2014) and rainfall erosivity during the melting season (i.e. spring). For adjustment of erosivity in spring we only used the projections from MIROC3.2_R2, as it is regarded as the best model ensemble for capturing daily precipitation compared to R1 and R3 (Ji et al. 2016).

Soil property projections for New South Wales (soil organic carbon) were obtained from DPIE (Gray & Bishop 2017) and used to calculate soil erodibility based on Yang et al. (2017). Other input data include soil texture from the Soil and Landscape Grid of Australia (Grundy et al. 2015) at a spatial resolution of 3 arc seconds (about 90 m), the 30 metre

Digital Elevation Model (DEM) (Shuttle Radar Topography Mission, SRTM), and the latest satellite-derived fractional vegetation cover (Version 3.0.2) at a spatial resolution of 500 metres and on a monthly basis since 2000 (Guerschman et al. 2009).

The extreme rainfall indices (ERIs)

Various ERIs were calculated from the NARClIM projections (Evans et al. 2014b) (Table 1). These ERIs represent annual accumulated precipitation (e.g. R95p and R99p), count days with extreme rainfall depth (e.g. R20mm and Rnnmm), and illustrate monthly rainfall variation (e.g. Rx1day and Rx5day).

Six ERIs (R20mm, Rnnmm, R95p, R99p, Rx1day and Rx5day) were selected to compare and assess their relationships with rainfall erosivity for each ensemble and period. These six indices were chosen because they are common and representative in time-steps. Note that only Rx1day and Rx5day are defined on a monthly basis, while all the other indices are defined on an annual basis; therefore, only Rx1day and Rx5day were applied to examine the seasonal rainfall extremes and their relationships with the rainfall erosivity and erosion rates.

Table 1 The selected six extreme rainfall indices and their definitions

| ERI | Description | Unit |
|--|---|------|
| R20mm | Annual counts of days with rainfall above 20 mm. Count the days where: $RR_{ij} \geq 20$ mm | days |
| Rnnmm | Annual counts of days with rainfall above 25 mm. Count the days where: $RR_{ij} \geq 25$ mm | days |
| Rx1day (monthly) | Daily maximum 1-day precipitation. $Rx1day_j = \max (RR_{ij})$ | mm |
| Rx5day (monthly) Rx5day_y (annually) | Maximum 5-day accumulated precipitation (annual and monthly). Let RR_{kj} be the precipitation amount for the 5-day interval ending k period j. $Rx5day_j = \max (RR_{kj})$ | mm |
| R95p | Accumulated precipitation from events above the 95 th percentile. Let RR_{wj} be the daily precipitation amount on a wet day w ($RR \geq 1.0$ mm) in period I and let RR_{wn95} be the 95 th percentile of precipitation on wet days in the period. If W represents the number of wet days in the period, then: $R95p_j = \sum_{w=1}^W RR_{wj}$ where $RR_{wj} > RR_{wn95}$ | mm |
| R99p | Accumulated precipitation from events above the 99 th percentile. Let RR_{wj} be the daily precipitation amount on a wet day w ($RR \geq 1.0$ mm) in period I and let RR_{wn99} be the 99 th percentile of precipitation on wet days in the period. If W represents the number of wet days in the period, then: $R99p_j = \sum_{w=1}^W RR_{wj}$ where $RR_{wj} > RR_{wn99}$ | mm |

Note: Let RR_{ij} be the daily precipitation amount on day i in period j

Rainfall erosivity

The rainfall erosivity model (equation (1), based on Yang et al. 2016):

$$\hat{E}_j = \alpha [1 + \eta \cos(2\pi f_j - \omega)] \sum_{d=1}^N R_d^\beta \quad (1)$$

where the rainfall erosivity (E) for month j is estimated from the daily rainfall amount R_d (mm day^{-1}); N represents the number of rain days in the month; α , β , η and ω are the model parameters. More information about the parameters and model is presented in Yang et al. (2016).

Snowfall in the Alpine region is common; however, it was neglected in previous studies (Yang & Yu 2015; Yang et al. 2016). It is believed that the exclusion of snowmelt in erosion modelling would result in underestimation of rainfall erosivity and erosion, particularly in the Alpine region and its surrounding areas. Studies of the impact of snowmelt on erosion have been conducted in other parts of the world; for example, Switzerland (Meusburger et al. 2014), Canada (Hayhoe et al. 1995) and Germany (Ollesch et al. 2006), but such research has not yet been done in Australia.

In this study, snowmelt was considered in simulating and calibrating the rainfall erosivity across the Alpine region in spring. The daily snowmelt was estimated from the models described in Bormann et al. (2014) and Rango and Martinec (1995):

$$Mp = k \cdot \frac{\rho_s}{\rho_w} \cdot (T_{mean} - T_{ref}) \quad (2)$$

where Mp is potential snowmelt (mm day^{-1}), ρ_s is snow density (g cm^{-3}) simulated based on multiple linear regression (MLR) and climate variables, ρ_w is water density (assumed to be 1 g cm^{-3}), T_{mean} refers to the daily mean temperature and T_{ref} is set to 0°C . The calculation of rainfall erosivity was adjusted by adding the snowmelt to the rainfall density using the daily rainfall erosivity model as presented in Yang et al. (2016) and equation (1) is rewritten as:

$$\hat{E}_j = \alpha[1 + \eta \cos(2\pi f_j - \omega)] \sum_{d=1}^N (R_d + Mp)^\beta \quad (3)$$

The daily rainfall amount R_d was calculated from the bias-corrected daily rainfall projections of all the 12 NARClIM ensembles; however, the snowmelt was only derived from the MIROC3.2_R2 as this model ensemble is more trustworthy in reproducing precipitation compare to R1 and R3 in terms of daily scale (Ji et al. 2016), while the performance of the four GCMs are similar.

Once the rainfall erosivity is estimated, the hillslope erosion can be calculated using RUSLE along with other factors, the slope-steepness factor (LS), groundcover (C) and the soil erodibility (K) (Renard et al. 1997):

$$A = R \cdot K \cdot LS \cdot C \cdot P \quad (4)$$

where A is the predicted soil loss ($\text{t ha}^{-1} \text{ yr}^{-1}$), R is rainfall erosivity ($\text{MJ mm ha}^{-1} \text{ hr}^{-1} \text{ yr}^{-1}$) as described above, K is the soil erodibility factor ($\text{t ha hr ha}^{-1} \text{ MJ}^{-1} \text{ mm}^{-1}$), LS represents the slope and steepness factor (unitless) estimated from DEM, and C is the cover and management (C) factor (unitless). The erosion control (P) factor (unitless) is not considered in this work.

The K factor was estimated based on Yang et al. (2017) using the recent digital soil maps and soil property projections including soil texture and organic matter (Grundy et al. 2015; Gray et al. 2016). The LS -factor was calculated from the 30 metre DEM (SRTM) based on a comprehensive method as described in Yang (2015). The C factor was estimated on a monthly basis and updated from the latest satellite-derived fractional vegetation cover (Version 3.0.2) (Guerschman et al. 2009) based on methods described in Yang (2014). The C factor was adjusted with snow cover in winter months (June, July, August – JJA) based on a snow mask prepared from the snow depth projection, and a specific value (0.0044) was assigned to the areas covered by snow.

Adequate random points (> 5000 for the entire study area and 1550 for the Alpine region) were used to sample ERI, rainfall erosivity and hillslope erosion rates for the baseline (1990 to 2009), near future (2020 to 2039) and far future (2060 to 2079) periods. These randomly sampled data were used for statistical analyses and identification of the relationship between rainfall extremes, erosivity and erosion.

Model performance is measured by the coefficient of efficiency, E_c (Nash & Sutcliffe 1970) as it is commonly used to assess model performance in hydrology and soil sciences (Loague & Freeze 1985; Risse et al. 1993):

$$E_c = 1 - \frac{\sum_{i=1}^M (y_i - \hat{y})^2}{\sum_{i=1}^M (y_i - \bar{y})^2} \quad (5)$$

where y_i are observed values while \hat{y} are modelled values; \bar{y} is the average of observed values, and M represented the sample size. Essentially, E_c is an indicator of how close the scatters of predicted versus actual values are to the 1:1 line (Yang & Yu 2015).

2.2 Quality control

We used RUSLE to estimate rainfall erosivity and hillslope erosion. All RUSLE factors were estimated based on the well-established and published methods as described in Section 2.1. All input data sets are published and come with a quality indicator.

The report was reviewed by internal and external reviewers, and followed the procedures as set out in DPIE's Scientific Rigour Position Statement (OEH 2013).

2.3 Data storage and access

All output data (time-series rainfall erosivity and erosion) were converted to raster format (ArcGIS ESRI grid) and supplied to the MCAS-S (Multi-Criteria Analysis Shell for Spatial Decision Support) datapacks for distribution and storage. All input data to the model and by-products are stored on hard disk drives. All data are in a coordinate system of GCS WGS84 at 0.001 degree (about 100 m). The extent of the datasets includes the MM region, ACT and SET with the boundary at top: -32.671254, left: 143.317445, right: 150.745676, and bottom: -37.505077.

To meet the naming limitation of ArcGIS we used a simple and short naming approach; for example, 'ero_2038' represents the projected mean hillslope erosion in 2038 from all model ensembles; and 'r_2038' represents the projected mean erosivity in 2038 from all model ensembles. Rather than use long file names with many repeating or redundant characters (such as previously used in the NARClIM project), we prefer short file names under well-structured folders (e.g. Alpine\erosion\2020_39\annual\ero_2038).

3. Results

3.1 Correlation between extreme rainfall indices and rainfall erosivity

Six ERI maps have been prepared for the study area, for the baseline (1990 to 2009), near future (2020 to 2039) and far future (2060 to 2079) periods. The impacts of ERIs on rainfall erosivity and erosion were assessed and compared using 5000 random points within the region. The relationship between the ERIs and the corresponding rainfall erosivity for each period is shown in Figure 2. Six ERIs at the annual step were compared to examine their correlation with rainfall erosivity (Figure 2a). Rx5day (annual step) is the most effective index; it has stronger correlation with rainfall erosivity for the baseline ($R^2=0.841$), near future ($R^2=0.842$) and far future ($R^2=0.827$) periods.

The impact of the corresponding ERIs on hillslope erosion (correlation < 0.3) is much less compared to that of rainfall erosivity (Figure 2b), since hillslope erosion is related to factors such as groundcover, soil property, slope steepness and length, but rainfall erosivity is predominately related to rainfall duration and intensity.

Both ERIs (Rx1day, Rx5day) have higher correlations with rainfall erosivity in summer (DJF) compared with other seasons (Table 2), possibly due to greater rainfall and higher intensity in summer. The projection in winter (JJA) and autumn (March, April, May – MAM) is less accurate (R^2 and E_c around 0.7). Rx5day has a slightly higher seasonal correlation with erosivity (and therefore erosion) than Rx1day in all periods (Table 2). On an annual basis,

the correlation between the mean annual erosivity (from all 12 ensembles) and Rx5day is stronger ($R^2 = 0.813$) and higher than any other ERI (Figure 3). Thus, Rx5day was selected to predict the erosivity and seasonal variation in this study.

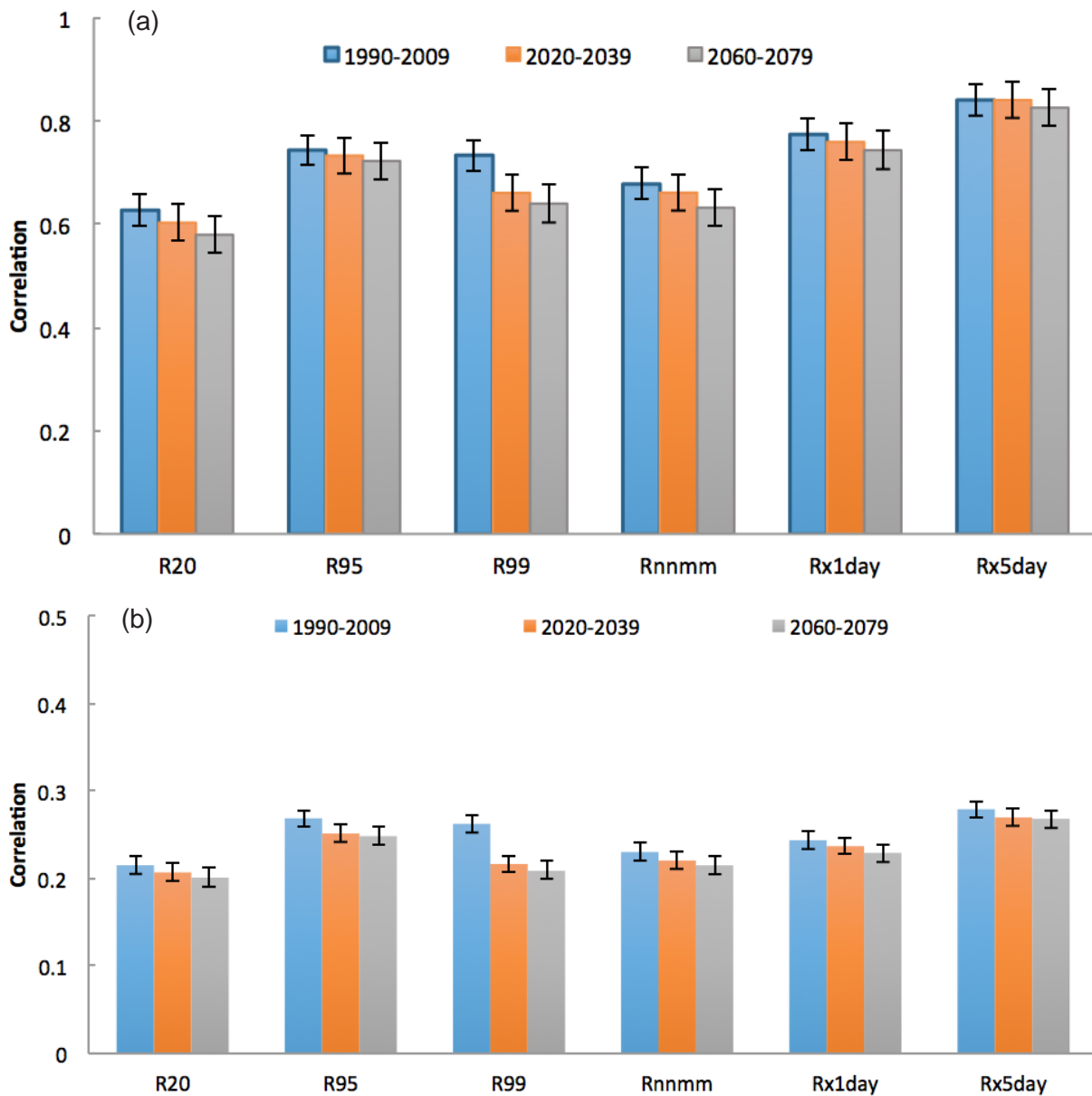


Figure 2 Correlation coefficients between different extreme rainfall indices (refer to Table 1) and rainfall erosivity (a) and erosion (b) for the baseline period (1990 to 2009), near future (2020 to 2039) and far future (2060 to 2079)

Table 2 Seasonal comparison between extreme rainfall indices, Rx1day and Rx5day, and their correlation with rainfall erosivity

| Correlation between ERI and erosivity | Baseline (1990 to 2009) | | Near future (2020 to 2039) | | Far future (2060 to 2079) | |
|---------------------------------------|-------------------------|--------|----------------------------|--------|---------------------------|--------|
| | Rx1day | Rx5day | Rx1day | Rx5day | Rx1day | Rx5day |
| DJF (summer) | 0.790 | 0.819 | 0.779 | 0.798 | 0.789 | 0.803 |
| MAM (autumn) | 0.725 | 0.766 | 0.701 | 0.750 | 0.672 | 0.715 |
| JJA (winter) | 0.790 | 0.802 | 0.783 | 0.801 | 0.758 | 0.778 |
| SON (spring) | 0.793 | 0.794 | 0.778 | 0.767 | 0.757 | 0.764 |

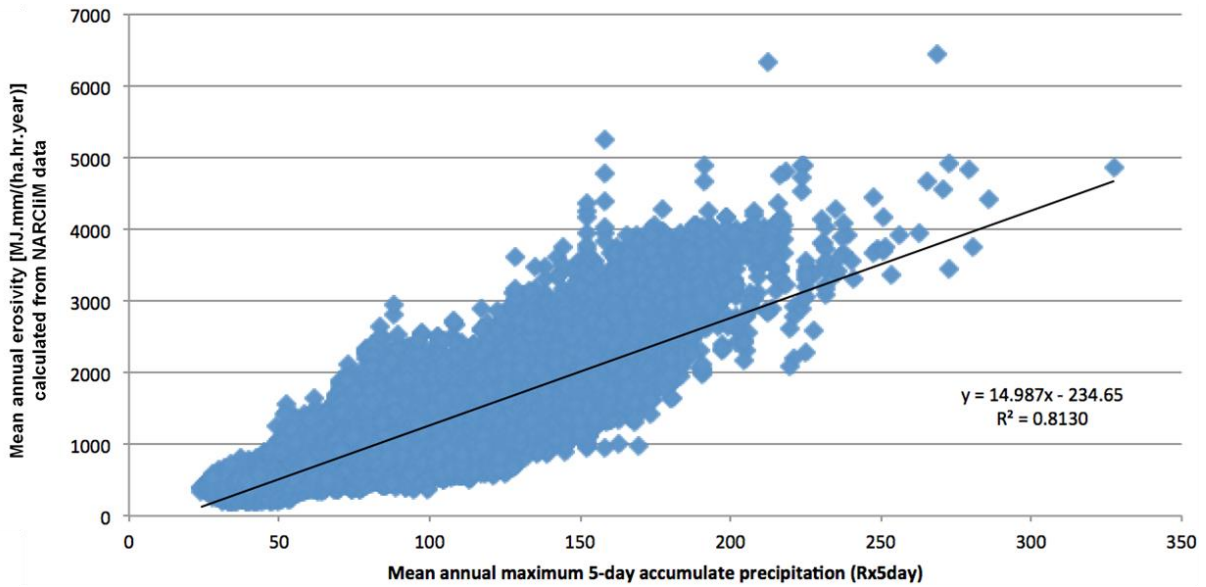


Figure 3 Relationship between mean annual erosivity and Rx5day index

3.2 Annual and seasonal rainfall erosivity

There is large spatial and seasonal variation in rainfall erosivity in the two projection periods across the Alpine region (Table 3, Figure 4). The SET region is projected to have higher rainfall erosivity in both near future and far futures (1121 and 1234 MJ mm ha⁻¹ hr⁻¹ yr⁻¹ respectively) though ACT has a slightly higher mean annual rainfall erosivity in the baseline period (1133 MJ mm ha⁻¹ hr⁻¹ yr⁻¹). SET is estimated to be at a higher risk in summer and autumn in the future. The ACT is projected to have higher rainfall erosivity in winter and spring, although still less than that from the Alpine region (Table 3). Like the Rx5day projected erosivity, summer is believed to be the season with highest rainfall erosivity, while winter always has the least across the study area in all three time periods. Moreover, the risk of rainfall erosivity generally tends to increase in both mean annual value and seasonal estimation across the study area.

Table 3 Annual and seasonal mean values of rainfall erosivity in the baseline, near future and far future periods across the study area

| Rainfall erosivity | Baseline (1990 to 2009) | | | | | Near Future (2020 to 2039) | | | | | Far Future (2060 to 2079) | | | | |
|--------------------|-------------------------|------|------|------------|--------|----------------------------|------|------|------------|--------|---------------------------|------|------|------------|--------|
| | MM | SET | ACT | Study area | Alpine | MM | SET | ACT | Study area | Alpine | MM | SET | ACT | Study area | Alpine |
| DJF | 249 | 504 | 503 | 334 | 326 | 308 | 554 | 515 | 389 | 376 | 289 | 593 | 477 | 389 | 382 |
| MAM | 134 | 274 | 250 | 180 | 206 | 126 | 287 | 208 | 178 | 179 | 212 | 333 | 312 | 252 | 272 |
| JJA | 61 | 83 | 110 | 69 | 171 | 55 | 59 | 100 | 57 | 164 | 75 | 68 | 124 | 73 | 172 |
| SON | 143 | 222 | 263 | 170 | 295 | 165 | 223 | 280 | 185 | 296 | 168 | 241 | 256 | 192 | 243 |
| ANN | 587 | 1082 | 1133 | 752 | 998 | 654 | 1121 | 1108 | 809 | 1015 | 743 | 1234 | 1175 | 905 | 1071 |

Note: DJF = summer, MAM = autumn, JJA = winter, SON = spring, ANN = annual

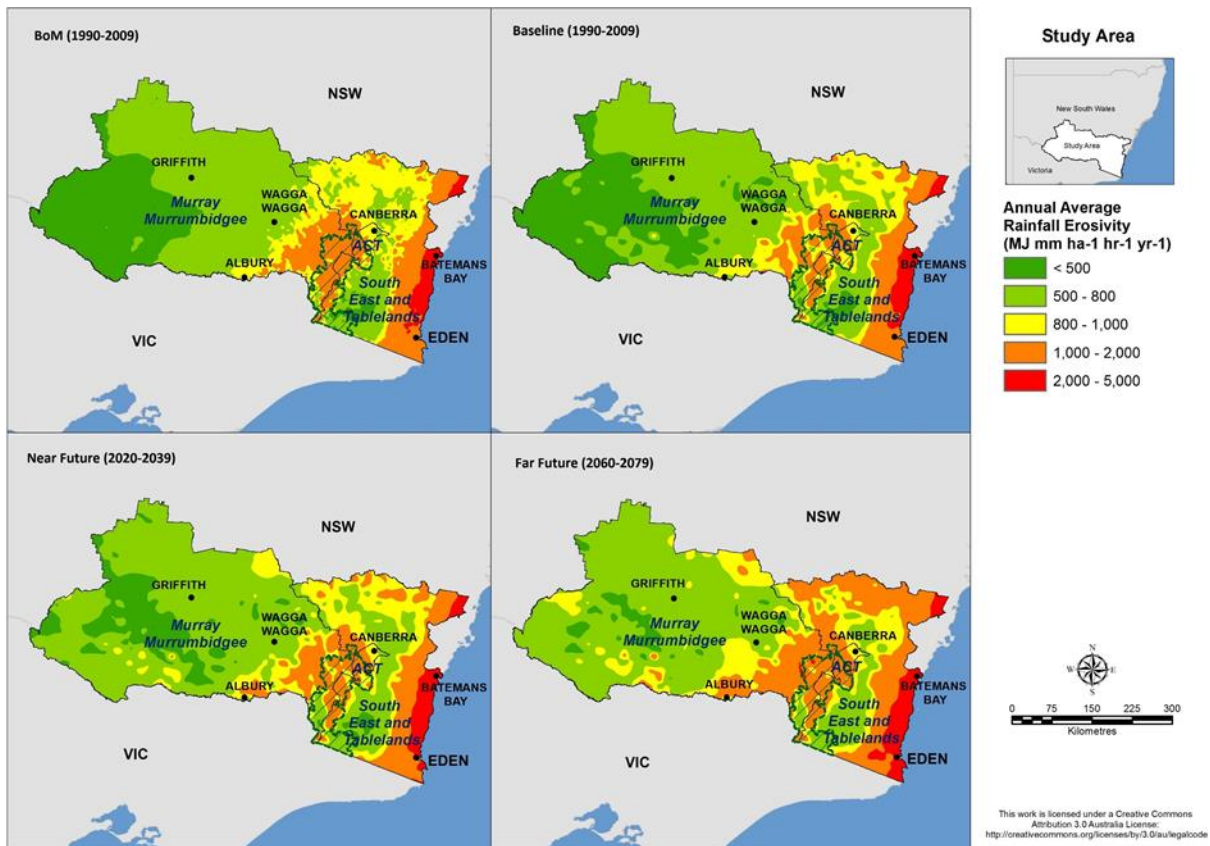


Figure 4 Mean annual rainfall erosivity in the baseline (1990 to 2009), near future (2020 to 2039) and far future (2060 to 2079) periods, compared with that calculated from BoM gridded rainfall in the 1990 to 2009 baseline period

3.3 Future change in rainfall erosivity

The future change in mean annual rainfall erosivity across the study area is shown in Figures 5 and 6. The changes for both projection periods are spatially heterogenous, ranging from around 50–60% in the near future in the western MM region to negative changes in the SET (Figure 5). Spatially similar but greater magnitude annual changes are apparent for the far future (Figure 6). The relative seasonal changes in rainfall erosivity range from an around 29% decrease in winter in SET in the near future (Figure 7) to an about 64% increase in autumn in the MM region in the far future (Figure 8), when compared to the baseline period.

Table 4 lists the details of the rainfall erosivity changes from the baseline period (1990 to 2009) to the near future (2020 to 2039) and far future (2060 to 2079). Green cells represent decreases in rainfall erosivity while the rest represent increases. Rainfall erosivity risk is projected to decrease over all three regions (MM, SET and ACT) in autumn and winter in the near future (Figure 7), but expected to increase in the far future (Figure 8).

In terms of the mean annual change, the rainfall erosivity is estimated to increase (9.7% on average) in the study area, except for some areas in the ACT (–2.15%). The rainfall erosivity in the Alpine region has a 2.22% increase in the near future and a further 8.31% increase in the far future. For seasonal changes, as much as a 20.79% increase occurs in summer, while about a 17% decrease across the study area is projected in winter in the near future. The largest change occurs in autumn (+51.73%) rather than summer (+17.89%) in the far future period. The SET area has greater seasonal variation in the near future (+10.57% in summer and -28.89% in winter) but the MM region is projected to have much more deviation in the far future (+64.27% in autumn and +19.44% in spring).

Table 4 Changes in mean annual and seasonal rainfall erosivity (%) in the near future (2020 to 2039) and far future (2060 to 2079)

Green cells indicate decreases in rainfall erosivity.

| Rainfall erosivity change | Change (%) in near future | | | | | Change (%) in far future | | | | |
|---------------------------|---------------------------|--------|--------|------------|-------------|--------------------------|--------|-------|------------|-------------|
| | MM | SET | ACT | Study area | Alpine | MM | SET | ACT | Study area | Alpine |
| DJF | 26.04 | 10.57 | 2.45 | 20.79 | 18.43 | 18.22 | 18.16 | -4.90 | 17.89 | 21.47 |
| MAM | -3.35 | -2.39 | -16.82 | -3.23 | -12.65 | 64.27 | 26.63 | 23.99 | 51.73 | 32.71 |
| JJA | -11.37 | -28.89 | -9.12 | -16.91 | -6.27 | 30.23 | -13.78 | 14.67 | 16.01 | -0.07 |
| SON | 16.72 | 3.55 | 6.05 | 12.38 | 1.53 | 19.44 | 10.39 | -1.72 | 16.26 | -15.27 |
| ANN | 13.00 | 3.22 | -2.15 | 9.68 | 2.22 | 28.63 | 15.83 | 3.73 | 24.21 | 8.31 |

Note: DJF = summer, MAM = autumn, JJA = winter, SON = autumn, ANN = annual

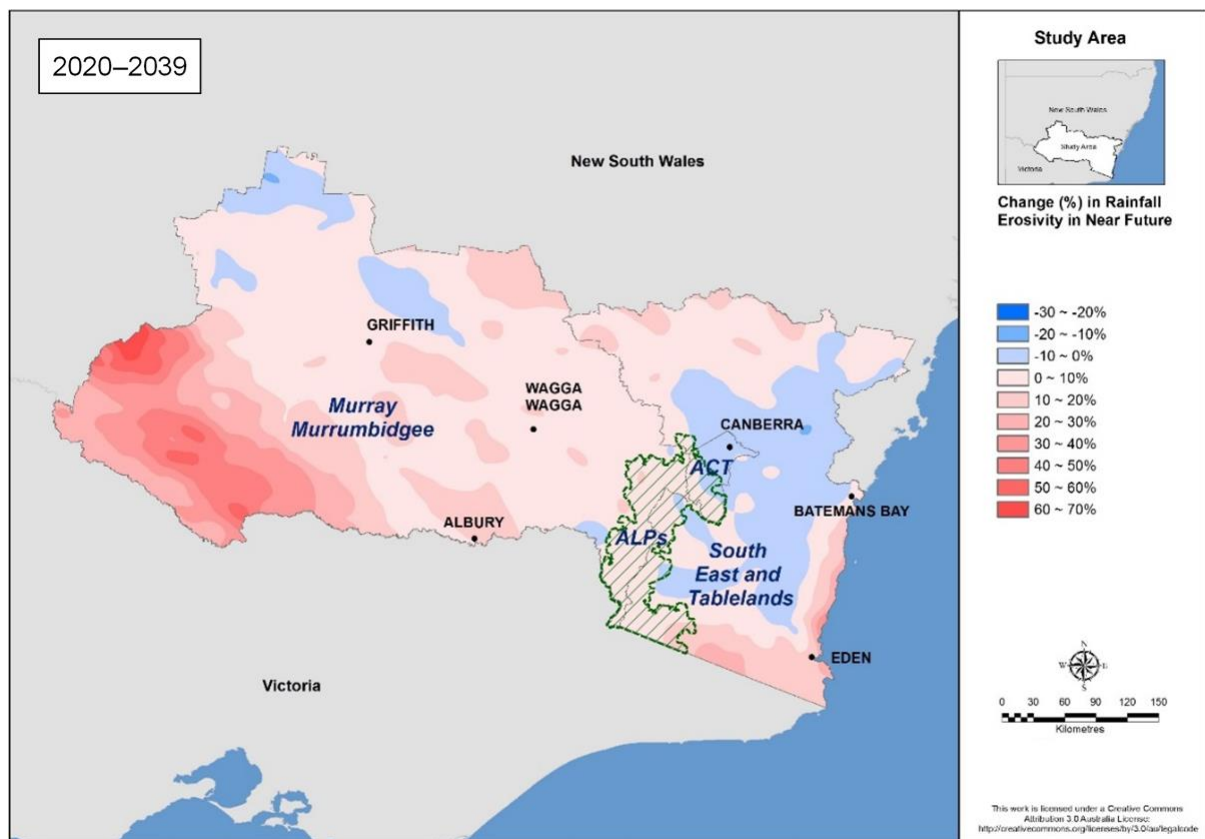


Figure 5 Changes in mean annual rainfall erosivity (%) in the near future (2020 to 2039) relative to the 1990 to 2009 baseline period

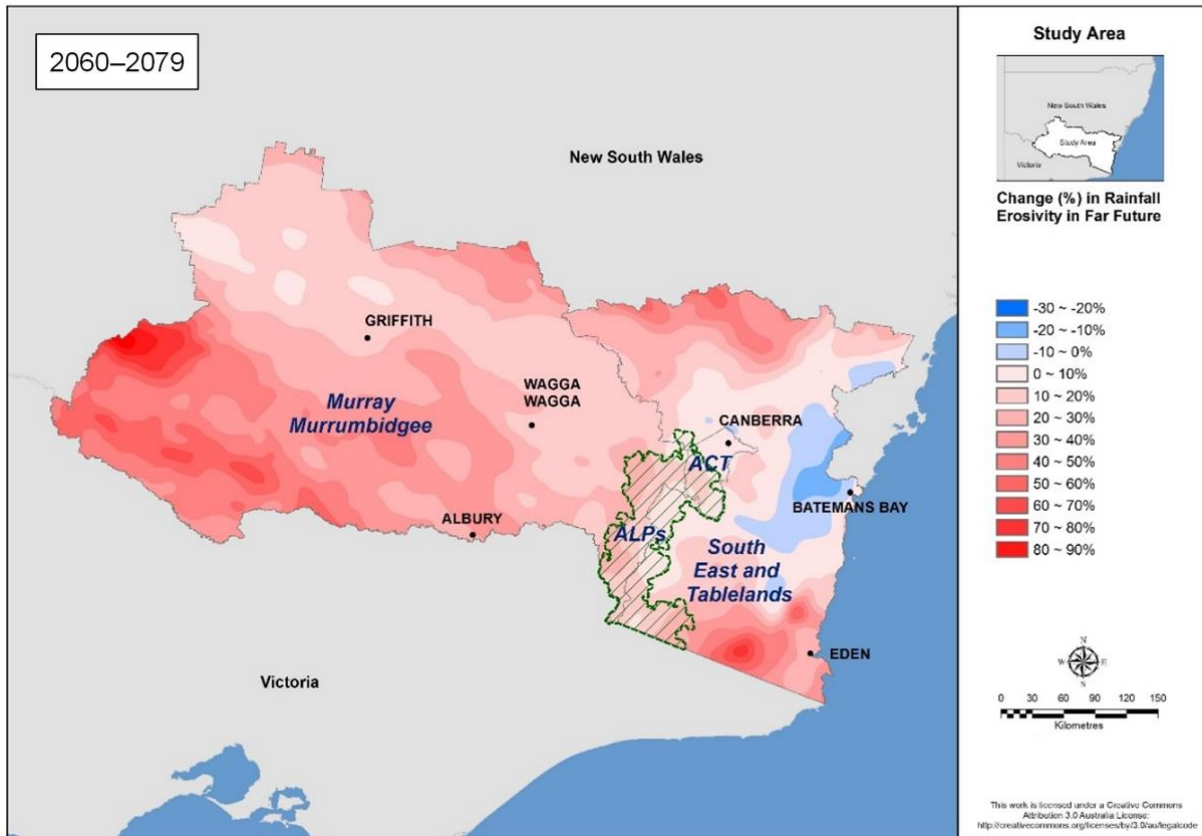


Figure 6 Changes in mean annual rainfall erosivity (%) in the far future (2060 to 2079) relative to the 1990 to 2009 baseline period

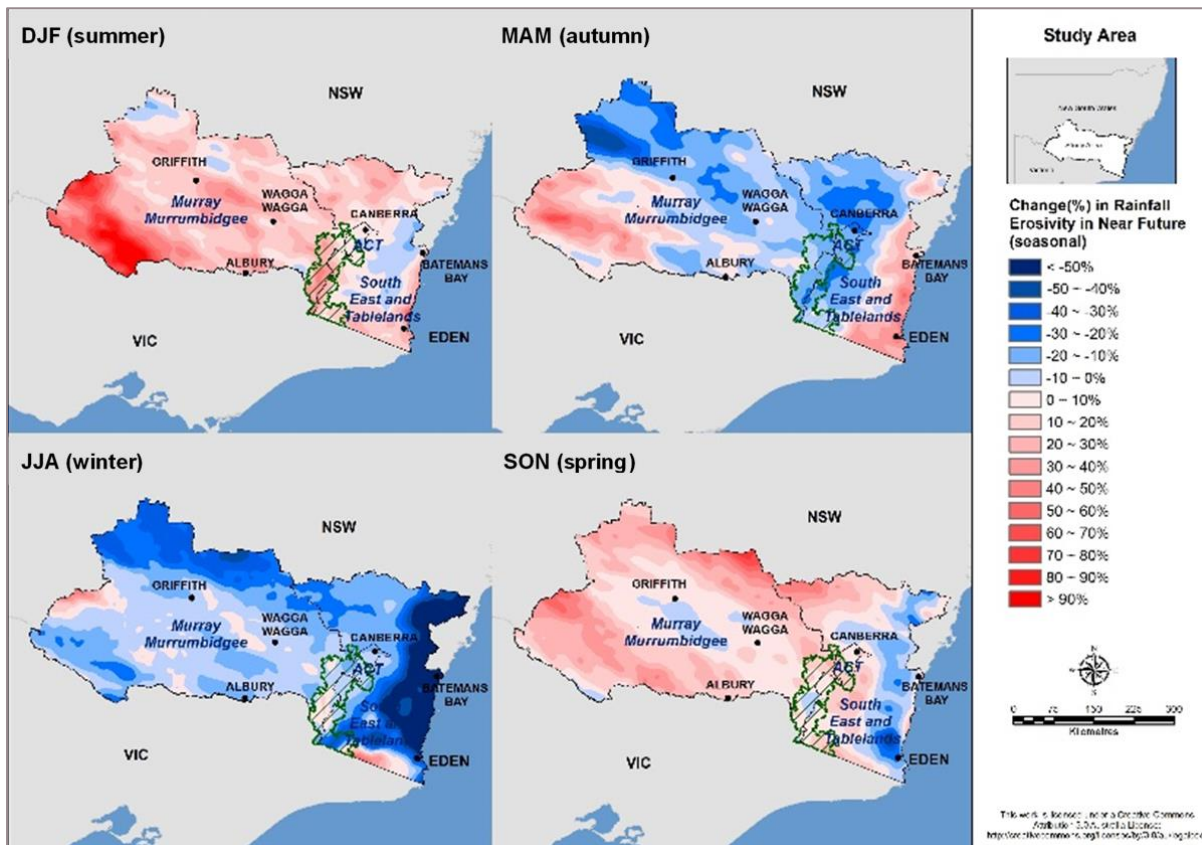


Figure 7 Changes in mean seasonal rainfall erosivity (%) in the near future (2020 to 2039) relative to the 1990 to 2009 baseline period

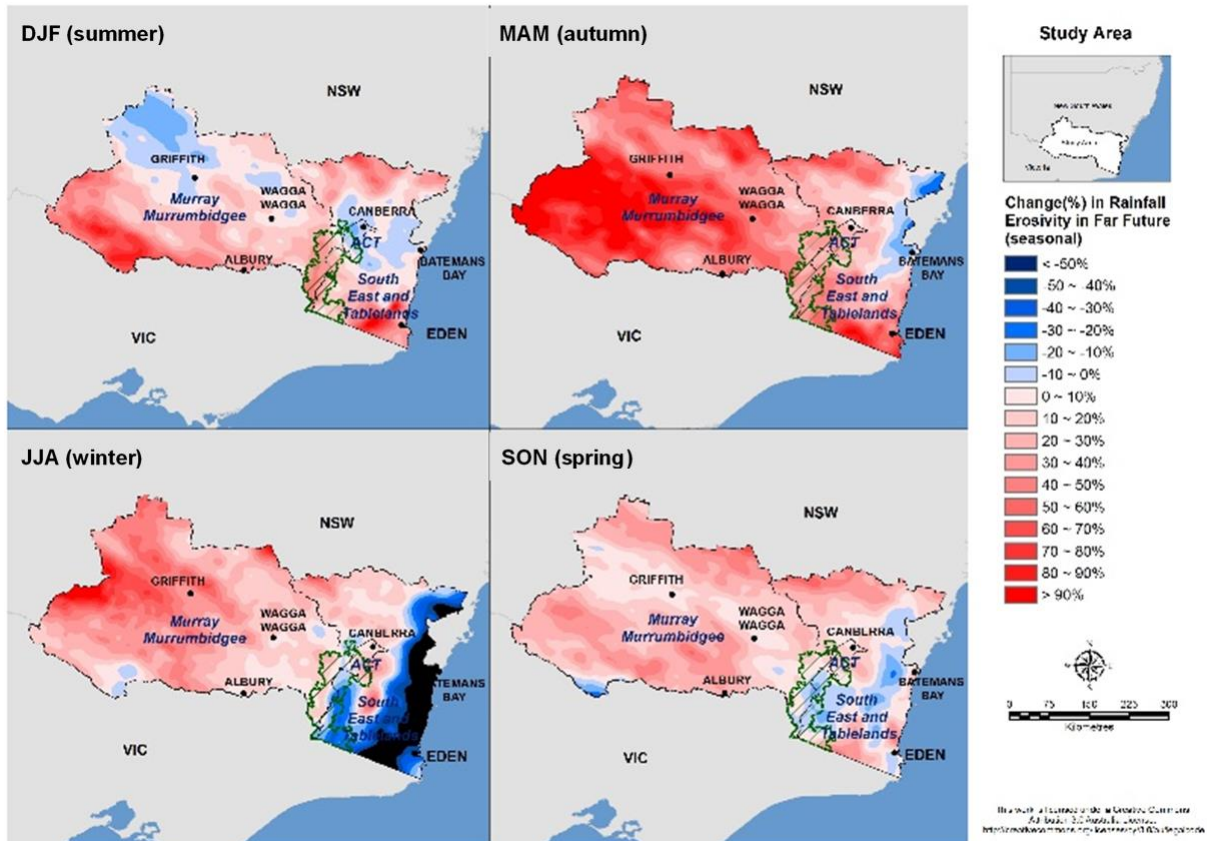


Figure 8 Changes in mean seasonal rainfall erosivity (%) in the far future (2060 to 2079) relative to the 1990 to 2009 baseline period

3.4 Impact of snowmelt on erosivity

Adding the snowmelt (mm day^{-1}) as additional rainfall (Loague & Freeze 1985; Risse et al. 1993) to the daily rainfall erosivity model (Yang & Yu 2015) resulted in greater variation in rainfall erosivity estimates in the Alpine region, especially in spring and October. To examine the snowmelt impact, rainfall erosivity estimates adjusted by snowmelt and rainfall (Equations (2)–(3)) from the 12 NARClIM ensembles were compared to those calculated from NARClIM rainfall projections without snowmelt (Yang et al. 2016). Figure 9 shows the per cent change in rainfall erosivity calculated with and without the snowmelt component for the three periods across the Alpine region. The snowmelt in spring increases the rainfall erosivity in the Alpine region by about 12% in the baseline period, 19% in the near future period, but there is almost nil (< 1%) impact in the far future owing to the projected temperature rise. On an annual basis, the snowmelt impact on mean annual rainfall erosivity is not obvious, with change being less than 3% in the baseline and near future periods, and nil (or negative) impact in the far future, as snowmelt mostly occurs in spring and has little impact on rainfall erosivity in other seasons.

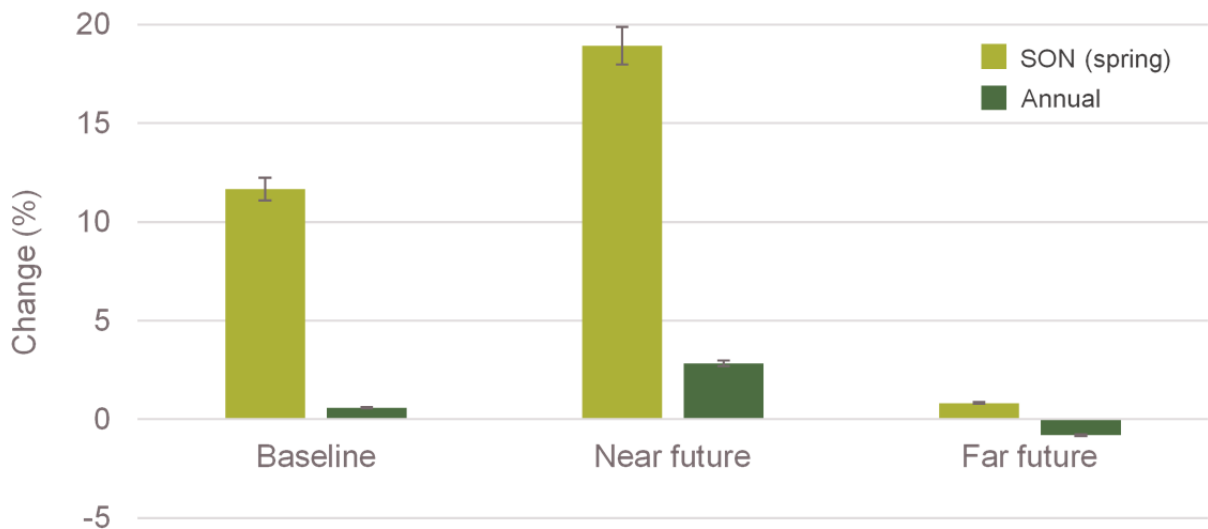


Figure 9 Projected change (%) in rainfall erosivity with and without snowmelt for the baseline (1990 to 2009), near future (2020 to 2039) and far future (2060 to 2079) periods

3.5 Hillslope erosion projection and changes

In general, hillslope erosion is projected to increase in the future with great variation in season and location. The high erosion risk area is projected to be in the ACT and SET in all periods. This includes some reserved areas such as Wadbilliga National Park, Monga National Park close to Batemans Bay and wilderness areas near Goobarragandra (Figure 10 to Figure 12).

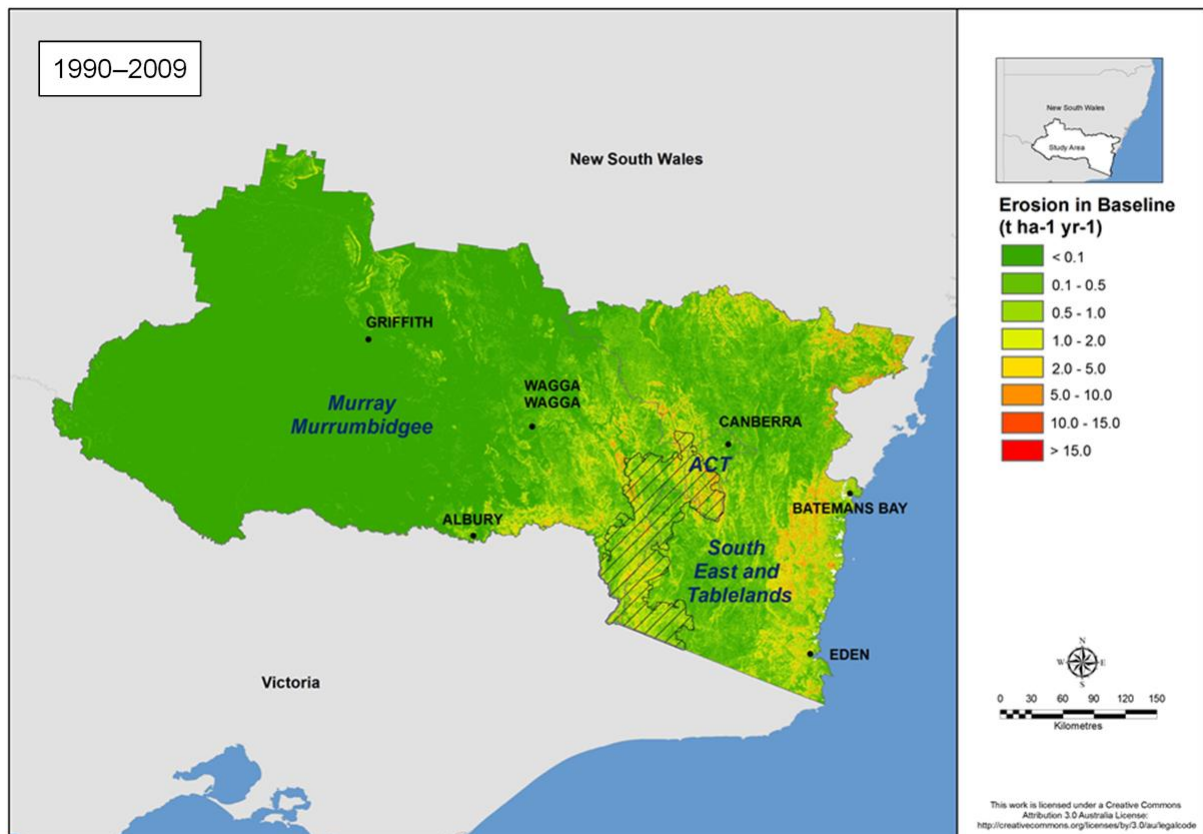


Figure 10 Projected hillslope erosion risk (t ha⁻¹ yr⁻¹) for the 1990 to 2009 baseline period

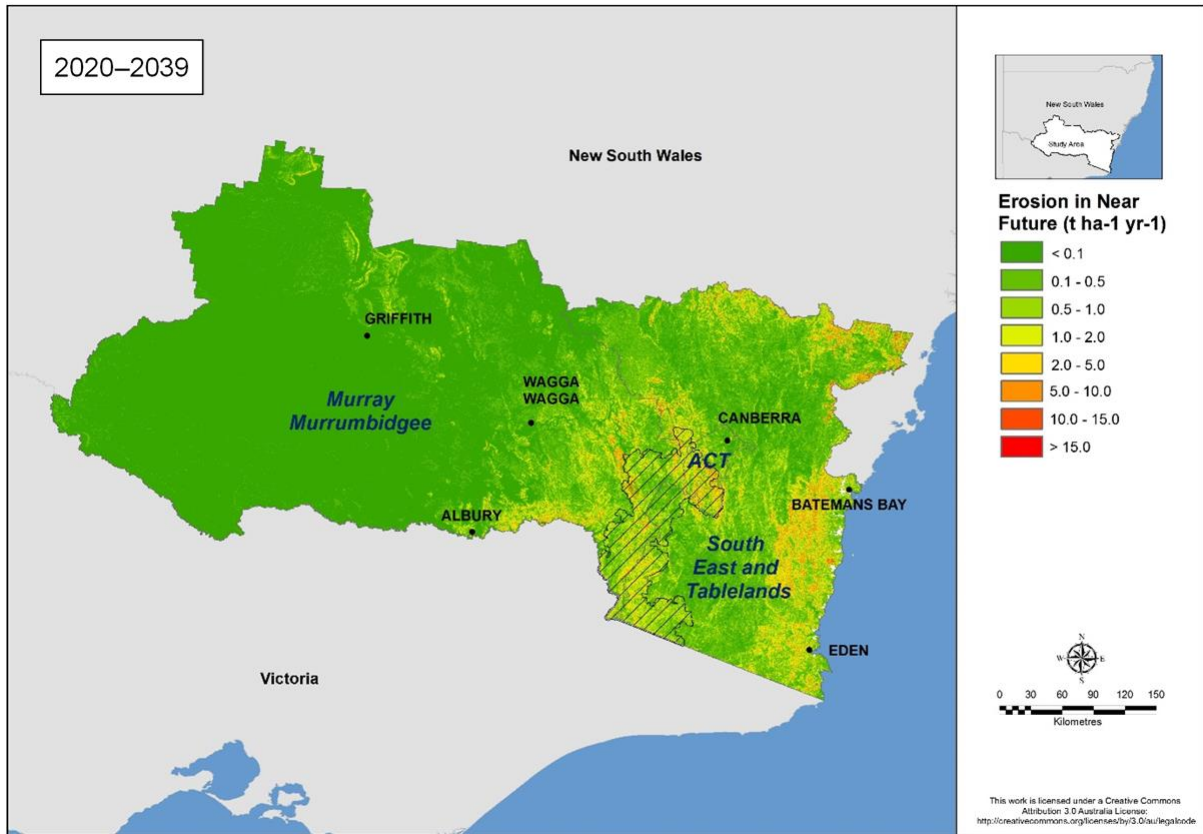


Figure 11 Projected hillslope erosion risk (t ha⁻¹ yr⁻¹) for the near future (2020 to 2039)

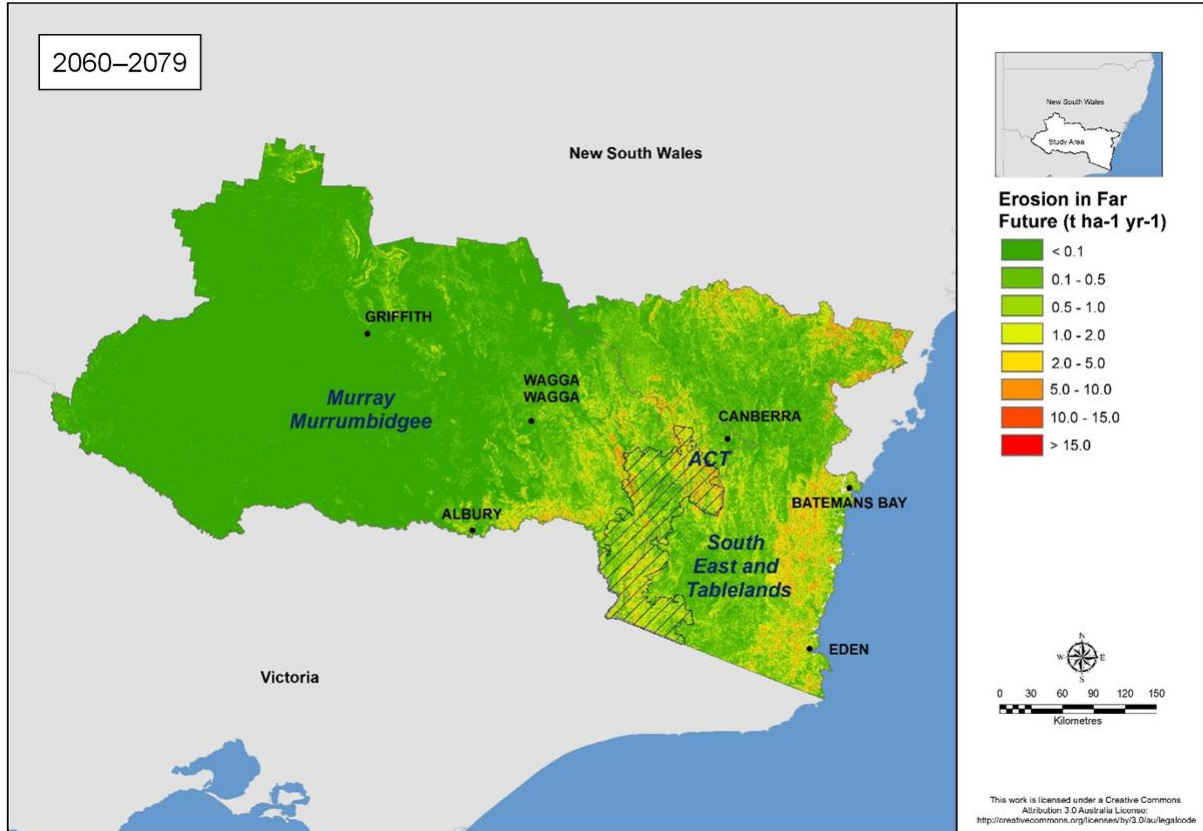


Figure 12 Projected hillslope erosion risk (t ha⁻¹ yr⁻¹) for the far future (2060 to 2079)

Table 5 shows the statistics of the annual erosion rates across the region in the baseline and future periods. From the estimated maximum values, the highest risk areas are located in SET, where erosion reaches 19.95 tonnes per hectare per year in the baseline period and slightly decreases in the near future (17.33 t ha⁻¹ yr⁻¹) and far future (19.85 t ha⁻¹ yr⁻¹). However, if the mean values are compared, the ACT (followed by the Alpine region) is likely to experience higher annual erosion than any other areas across the study area, where the mean annual erosion is 1.36 tonnes per hectare per year in the baseline period. There is little change projected in the near future (1.40 t ha⁻¹ yr⁻¹) and increases to 1.54 tonnes per hectare per year projected for the far future.

Table 5 Mean and maximum annual erosion values (t ha⁻¹ yr⁻¹) across the study area in the baseline (1990 to 2009), near future (2020 to 2039) and far future (2060 to 2079) periods

| Erosion (t ha ⁻¹ yr ⁻¹) | Baseline (1990 to 2009) | | Near future (2020 to 2039) | | Far future (2060 to 2079) | |
|--|-------------------------|------|----------------------------|------|---------------------------|------|
| | MAX | MEAN | MAX | MEAN | MAX | MEAN |
| MM | 14.16 | 0.16 | 14.81 | 0.17 | 17.08 | 0.19 |
| SET | 19.95 | 0.79 | 17.33 | 0.83 | 19.85 | 0.92 |
| ACT | 10.54 | 1.36 | 10.32 | 1.40 | 11.56 | 1.54 |
| Study area | 19.95 | 0.37 | 17.33 | 0.40 | 19.85 | 0.44 |
| Alpine | 12.30 | 1.14 | 12.89 | 1.20 | 13.99 | 1.30 |

Table 6 presents the change (%) in mean annual erosion from the baseline to future periods in the study area. SET is likely to experience greater variation in erosion change in the near future, where mean change is +18.76% in summer and the minimum change is -23.69% in winter. In the far future, more variation in erosion change is projected for the MM region (+69.11% in autumn and +21.70% in spring). Summer is the most vulnerable season with the highest change to the future periods compared to the other seasons.

Table 6 Changes (%) in mean annual and seasonal erosion values across the study area in the near future (2020 to 2039) and far future (2060 to 2079)

| Erosion change | Change in near future (%) | | | | | Change in far future (%) | | | | |
|----------------|---------------------------|--------|--------|------------|-------------|--------------------------|-------|-------|------------|--------------|
| | MM | SET | ACT | Study area | Alpine | MM | SET | ACT | Study area | Alpine |
| DJF | 27.72 | 18.76 | 9.24 | 24.62 | 24.79 | 21.01 | 30.47 | 5.93 | 23.81 | 33.28 |
| MAM | -3.30 | 4.66 | -11.73 | -0.89 | -7.81 | 69.11 | 40.43 | 39.57 | 59.60 | 48.13 |
| JJA | -9.45 | -23.69 | -3.60 | -13.89 | -2.10 | 35.43 | -4.99 | 26.85 | 22.48 | 7.18 |
| SON | 19.53 | 11.00 | 13.68 | 16.74 | 7.39 | 21.70 | 21.48 | 11.12 | 21.48 | -6.34 |
| ANN | 15.74 | 10.95 | 4.55 | 14.07 | 7.91 | 31.31 | 27.87 | 15.56 | 30.00 | 18.16 |

Note: DJF = summer, MAM = autumn, JJA = winter, SON = spring, ANN = annual

As estimated from the RUSLE model, the ACT has the highest risk of hillslope erosion rather than the Alpine region (Figure 13). Though the Alpine region (a mountainous region) has the highest LS-factor, the K-factor and C-factor are relatively low compared to those from the other parts of study area (MM and SET) (Figure 14). It is projected that the ACT has higher values in the K-factor, C-factor and LS-factor. These factors, along with the adjusted rainfall erosivity factor, result in the highest erosion in the ACT. Despite higher K and C values in the MM region, the corresponding hillslope erosion is projected to be very low since the area is flat and the LS values are very low.

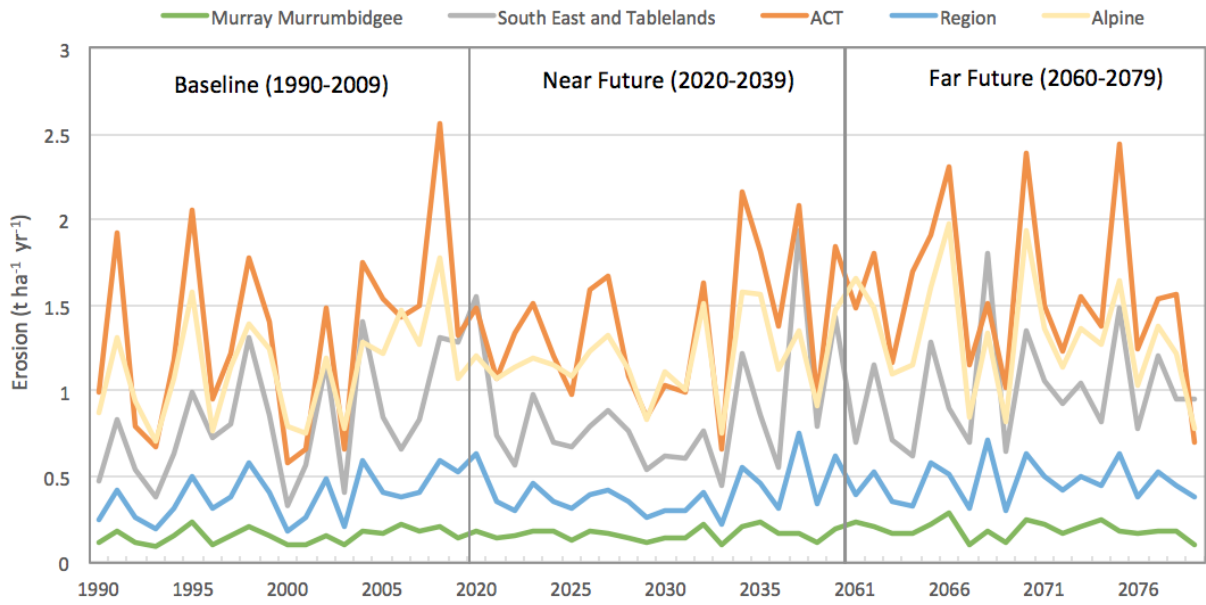


Figure 13 Projected hillslope erosion risk across the study area for the baseline (1990 to 2009), the near future (2020 to 2039) and the far future (2069 to 2079) periods

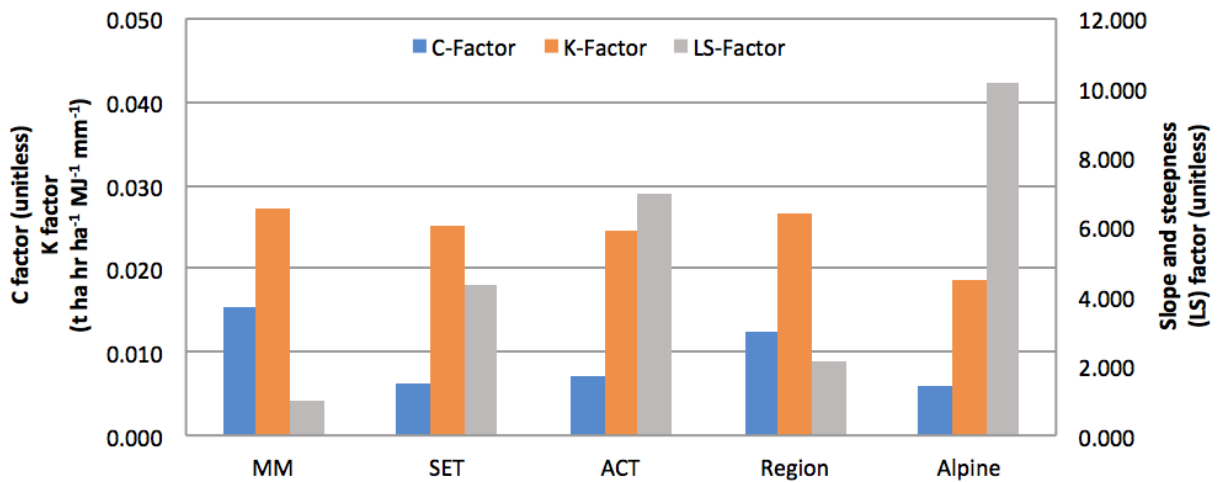


Figure 14 The C, K and LS factors of RUSLE across the study area

4. Discussion

4.1 Extra rainfall erosivity in spring

The impact of snowmelt on rainfall erosivity and erosion needs to be considered in the Alpine region in the baseline and near future periods. The snowmelt in spring can increase erosivity by 24% in the Alpine region; however, with the projected temperature rise and snow cover decreasing, the snowmelt impact on erosivity and erosion can largely be ignored in the far future.

4.2 High risk areas

The highest erosion risk area is projected to be in the ACT, followed by SET. The high erosion risk in these areas is due to the combined effects of steep lands and intense rainfall, as well as snowmelt. This highlights the importance of groundcover maintenance and soil management in these regions.

4.3 Limitations and further research

The following factors influence the accuracy of these outcomes:

- Daily NARClIM GCM/RCM projections (rainfall, snow, temperature) are at a spatial resolution of approximately 10 kilometres. This is considered a relatively coarse resolution and is a limiting factor in local ecosystem (erosion) modelling.
- Only one model ensemble was used to consider snowmelt impact on erosivity. This model might be biased, though it has been shown to be the most suitable model for this region.
- Further investigation into snow impacts on groundcover and erosivity is required. More model ensembles need to be used to remove biases and increase robustness.

5. Conclusion

Extreme rainfall has a significant impact on erosivity and erosion. Extreme rainfall indices can be used as indicators for potential hillslope erosion risk and to predict erosivity; however, the relationships vary among seasons and locations. Predictions in summer are likely to be more reliable than other seasons due to higher correlations and coefficients of efficiency.

The impact of snowmelt on rainfall erosivity and erosion needs to be considered in the Alpine region for both the baseline and near future periods. The snowmelt in spring can increase the erosivity by about 13–24% in the Alpine region; however, with the projected temperature rise and projected decreases in snow cover, the snowmelt impact on erosivity and erosion can largely be ignored in the far future.

The high erosion risk area is projected to be in the ACT, followed by the Alpine region if the mean erosion rates are considered. The high erosion risk is due to the combined effects of steep lands and intense rainfall, as well as snowmelt. This highlights the importance of groundcover maintenance and soil management in these regions. Rainfall erosivity and hillslope erosion in the study area are projected to increase by around 10% and 14%, respectively, in the near future (2020 to 2039), increasing by a further 24% and 30%, respectively, in the far future (2060 to 2079). These increases are expected to occur even if the groundcover is maintained at the current level.

This research was the first attempt to use snow data and projections to adjust erosivity in models to factor in hillslope erosion modelling. The methodology has been developed and applied in the Alpine region, with potential to be used globally.

6. References

- Alexander LV, Hope P, Collins D, Trewin B, Lynch A and Nicholls N 2007, Trends in Australia's climate means and extremes: a global context, *Australian Meteorological Magazine*, vol.56, pp.1–18.
- Bormann KJ, Evans JP and McCabe MF 2014, Constraining snowmelt in a temperature-index model using simulated snow densities, *Journal of Hydrology*, vol.517, pp.652–667.
- Cruse R, Flanagan D, Frankenberger J, Gelder B, Herzmann D, James D, Krajewski W, Kraszewski M, Laflen J, Opsomer J and Todey D 2006, Daily estimates of rainfall, water runoff, and hillslope erosion in Iowa, *Journal of soil and water conservation*, vol.61, pp.191–199.
- CSIRO and BoM 2015, *Climate Change in Australia Information for Australia's Natural Resource Management Regions: Technical Report*, CSIRO and Bureau of Meteorology, Australia.
- Di Luca AJ, Evans P and Ji F 2018, Australian snowpack in the NARClIM ensemble: evaluation, bias correction and future projections, *Climate Dynamics*, vol.51, no.1–2, pp.639–666.
- Evans JP, Ekstrom M and Ji F 2012, Evaluating the performance of a WRF physics ensemble over South-East Australia, *Climate Dynamics*, vol.39, no.6, pp.1241–1258.
- Evans JP, Ji F, Abramowitz G, Ekstrom M 2013a, Optimally choosing small ensemble members to produce robust climate simulations, *Environmental Research Letters*, vol.8.
- Evans JP, Fita L, Argüeso D and Liu Y 2013b, Initial NARClIM evaluation, in Piantadosi J, Anderssen RS and Boland J (eds), *MODSIM2013, 20th International Congress on Modelling and Simulation*, Modelling and Simulation Society of Australia and New Zealand, December 2013, pp.2765–2771.
- Evans J, Ji F, Lee C, Smith P, Argüeso D and Fita L 2014a, Design of a regional climate modelling projection ensemble experiment–NARClIM, *Geoscientific Model Development*, vol.7, pp.621–629.
- Evans JP, Argüeso D, Olson R and Di Luca A 2014b, 'NARClIM extreme precipitation indices report', NARClIM technical note 6, report to the NSW Office of Environment and Heritage, Sydney Australia, pp.109.
- Evans JP, Argüeso D, Olson R and Di Luca A 2017, Bias-corrected regional climate projections of extreme rainfall in south-east Australia, *Theoretical and Applied Climatology*, vol.130, nos3–4, pp.1085–1098.
- Fita L, Evans JP, Argüeso D, King AD and Liu Y 2016, Evaluation of the regional climate response to large-scale modes in the historical NARClIM simulations, *Climate Dynamics*, pp.1–15, doi: 10.1007/s00382-016-3484-x.
- Gray JM and Bishop TFA 2017, *Climate change impacts on three key soil properties in NSW*, Technical Report, NSW Office of Environment and Heritage, Sydney.
- Gray JM, Thomas FA, Bishop TFA and Wilford JR 2016, Lithology and soil relationships for soil modelling and mapping, *Catena*, vol.147, pp.429–440.
- Grundy MJ, Viscarra RA, Searle RA, Searle RD, Wilson PL, Chen C and Gregory LJ 2015, Soil and Landscape Grid of Australia, *Soil Research*, vol.53, no.8, pp.835–844.
- Guerschman JP, Hill MJ, Renzullo LJ, Barrett DJ, Marks AS and Botha EJ 2009, Estimating fractional cover of photosynthetic vegetation, nonphotosynthetic vegetation and bare soil in the Australian tropical savanna region upscaling the EO-1 Hyperion and MODIS sensors, *Remote Sensing of Environment*, vol.113, pp.928–945.
- Hayhoe H, Pelletier R and Coote D 1995, Estimating snowmelt runoff erosion indices for Canada, *Journal of Soil and Water Conservation*, vol.50, pp.174–179.

- Hughes L 2011, Climate change and Australia: key vulnerable regions, *Regional Environmental Change*, vol.11, no.1, pp.189–195.
- IPCC 2000, Special Report on Emissions Scenarios: A Special Report of Working Group III of the Intergovernmental Panel on Climate Change, published for the Intergovernmental Panel on Climate Change by Cambridge University Press, Cambridge, UK.
- Ji F, Ekstrom M, Evans JP and Teng J 2014, Evaluating rainfall patterns using physics scheme ensembles from a regional atmospheric model, *Theoretical and Applied Climatology*, vol.115, pp.297–304.
- Ji F, Evans JP, Teng J, Scorgie Y, Argüeso D and Di Luca A 2016, Evaluation of long-term precipitation and temperature WRF simulations for southeast Australia, *Climate Research*, vol.67, pp.99–115, DOI 10.3354/cr01366.
- Loague KM and Freeze RA 1985, A comparison of rainfall-runoff modeling techniques on small upland catchments, *Water Resources Research*, vol.21, pp.229–248.
- Meusburger K, Leitinger G, Mabit L, Mueller M, Walter A and Alewell C 2014, Hillslope erosion by snow gliding—a first quantification attempt in a subalpine area in Switzerland, *Hydrology and Earth System Sciences*, vol.18, pp.3763–3775.
- Nash JE and Sutcliffe JV 1970, River flow forecasting through conceptual models part I—A discussion of principles, *Journal of Hydrology*, vol.10, pp.282–290.
- Nearing MA, Pruski FF and O’ne MR 2004, Expected climate change impacts on hillslope erosion rates: A review, *Journal of Soil and Water Conservation*, vol.59, no.1, pp.43–50.
- OEH 2013, *Scientific Rigour Position Statement*, NSW Office of Environment and Heritage, www.environment.nsw.gov.au/-/media/OEH/Corporate-Site/Documents/Research/Our-science-and-research/oeh-scientific-rigour-position-statement-2013.pdf.
- Ollersch G, Kistner I, Meissner R and Lindenschmidt KE 2006, Modelling of snowmelt erosion and sediment yield in a small low-mountain catchment in Germany, *Catena*, vol.68, pp.161–176.
- Rango A and Martinec J 1995, Revisiting the degree-day method for snowmelt computations, *Journal of the American Water Resources Association*, vol.31, pp.657–669.
- Renard KG, Foster GR, Weesies G, McCool D and Yoder D 1997, *Predicting hillslope erosion by water: a guide to conservation planning with the Revised Universal Soil Loss Equation (RUSLE)*, US Government Printing Office Washington, DC.
- Risse L, Nearing M, Laflen J and Nicks A 1993, Error assessment in the universal soil loss equation, *Soil Science Society of America Journal*, vol.57, pp.825–833.
- Skamarock WC, Klemp JB, Dudhia J, Gill DO, Barker DM, Duda MG, Huang XY, Wang W and Powers JG 2008, *A description of the advanced research WRF Version 3*, NCAR Technical Note, National Center for Atmospheric Research, Boulder Colorado, USA.
- Yang X 2014, Deriving RUSLE cover factor from time-series fractional vegetation cover for hillslope erosion modelling in New South Wales, *Soil Research*, vol.52, pp.253–261.
- Yang X 2015, Digital mapping of RUSLE slope length and steepness factor across New South Wales, Australia, *Soil Research*, vol.53, pp.216–225.
- Yang X and Yu B 2015, Modelling and mapping rainfall erosivity in New South Wales, *Soil Research*, vol.53, pp.178–189.
- Yang X, Yu B, Zhu Q and Liu D 2016, Predicting Changes of Rainfall Erosivity and Hillslope Erosion across New South Wales, Australia, *Journal of Earth Science Climate Change*, vol.7, no.3, p.2.
- Yang X, Gray J, Chapman C, Zhu Q, Tulau M and McInnes-Clarke S 2017, Digital mapping of soil erodibility for water erosion in New South Wales, Australia, *Soil Research*, vol.56, no.2, pp.158–170.